Supplementary material for "Climate sensitivity of the summer runoff of two glacierised Himalayan catchments with contrasting climate"

Sourav Laha[1,2], Argha Banerjee[1], Ajit Singh[2], Parmanand Sharma[2], and Meloth Thamban[2]

[1]Earth and Climate Science, Indian Institute of Science Education and Research (IISER) Pune, Pune-411008, India
[2]National Centre for Polar and Ocean Research (NCPOR), Ministry of Earth Sciences, Vasco-da-Gama, Goa-403804, India

Correspondence: Argha Banerjee (argha@iiserpune.ac.in)

Table S1. Details of the hydrometeorological observations used in this study. All hydro-meteorological data of upper Dudhkoshi catchment (Chevallier et al., 2017) are accessible from http://www.papredata.org/.

Parameters (station name)	Sensor	Accuracy (Range)	Data availability
Chandra catchment (Pratap et al., 2019; Singh et al., 2020)			
Runoff (Tandi)	YSI radar	$\pm$ 2 mm	26Th June, 2016 to 30th Oct, 2018 (with gaps)
Precipitation (Himansh)	OTT Pluvio precipitation bucket	$\pm$ 0.05 mm	18th Oct, 2015 to 5th Oct, 2018 (with gaps)
2m air temperature (Himansh)	Campbell HC2S3	$\pm 0.1^{\circ}$C (-50 to + 60 $^{\circ}$C)	18th Oct, 2015 to 5th Oct, 2018 (with gaps)
Incoming shortwave radiation (Himansh)	Kipp and Zonen four component net radiometer	$< 5\%$–day total (305–2800 nm, 0–2000 Wm^{-2})	18th Oct, 2015 to 5th Oct, 2018 (with gaps)
Upper Dudhkoshi catchment (Chevallier et al., 2017; Sherpa et al., 2017)			
Runoff (Phadking)	Campbell sensor (details not available)		7th April 2010 to 16th April 2017
Precipitation (Phadking)	Campbell sensor (details not available)		7th April 2010 to 23th April 2017 (with gaps)
2m air temperature (Phadking)	Campbell sensor (details not available)		7th April 2010 to 23th April 2017 (with gaps)
2m air temperature (Changri Nup)	Vaisala HMP45C	$\pm 0.2^{\circ}$C	1st Nov, 2010 to 30th Nov, 2014
Incoming shortwave radiation (Changri Nup)	Kipp and Zonen CNR4	$\pm$3%–day total (0.305–2.8 μm)	1st Nov, 2010 to 30th Nov, 2014

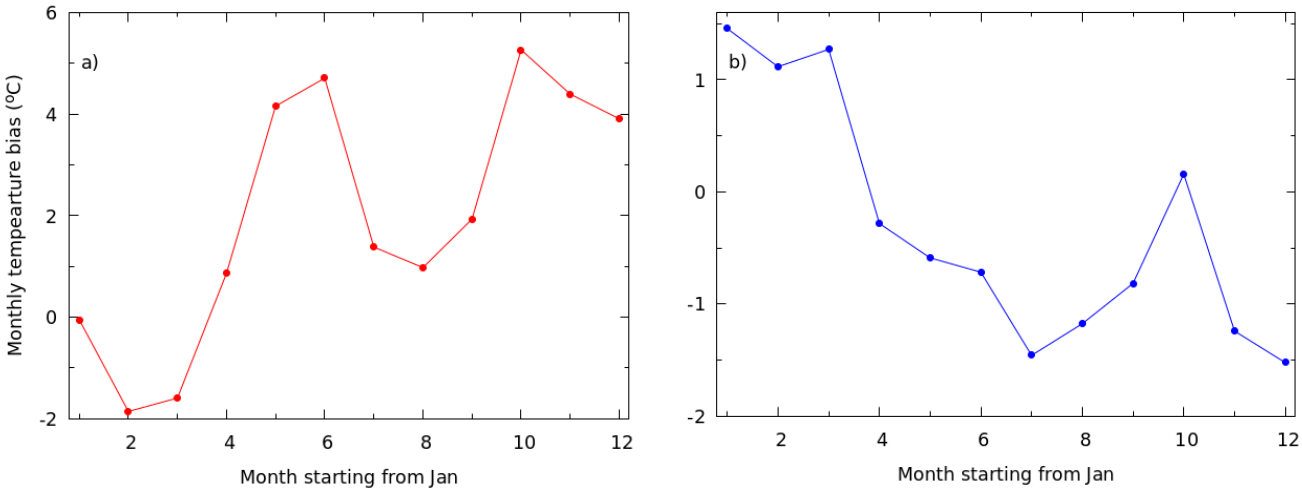

Figure S1. Mean monthly bias in ERA5 2m air temperature for (a) Chandra, and (b) upper Dudhkoshi catchments with respect to the corresponding stations (Himansh and Phadking, respectively).

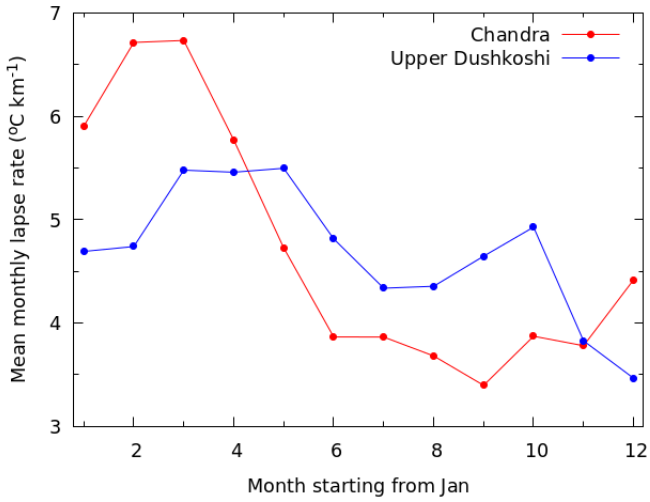

Figure S2. The mean monthly temperature lapse rates for Chandra (red symbols + line) and upper Dudhkoshi (blue symbols + line) catchments.

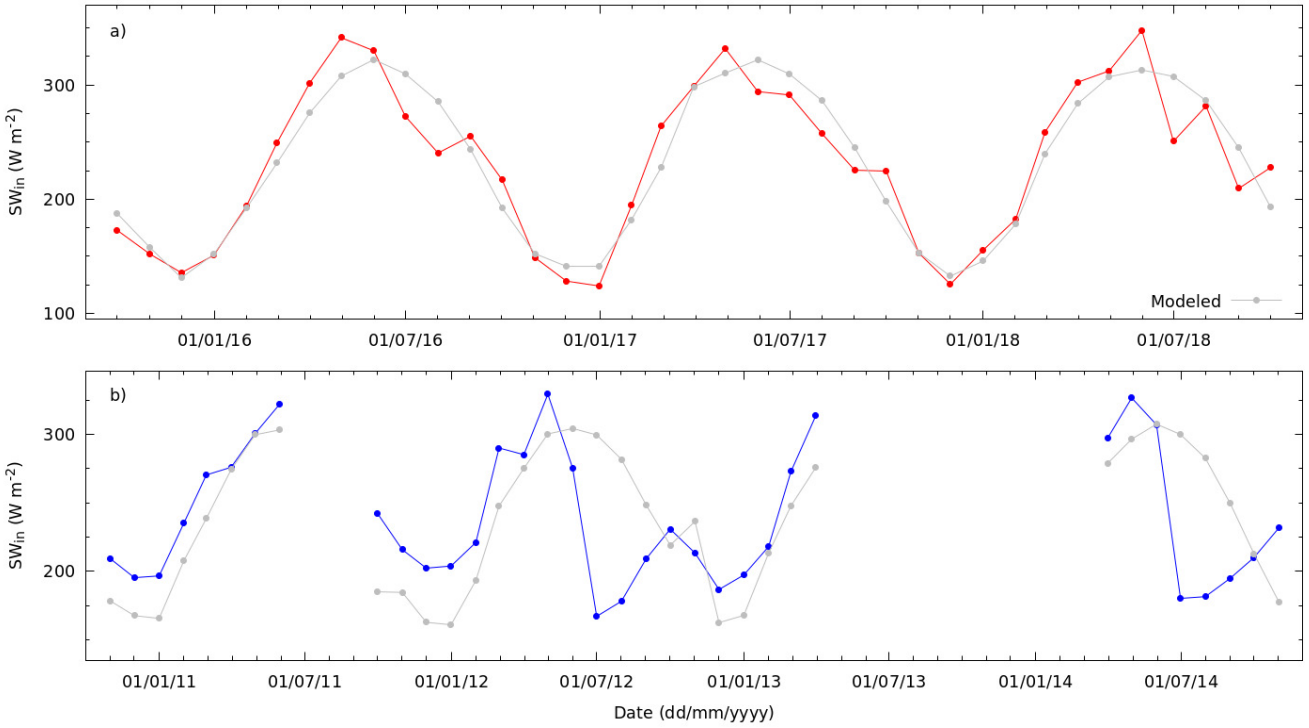

Figure S3. The incoming shortwave radiation (SW_{in}) estimated by VIC model was scaled so that it matched that observed at Himansh (Chandra catchment) and Changri Nup (upper Dudhkoshi catchment). In this plot, monthly modelled SW_{in} (gray lines + symbols) were shown for (a) Chandra, and (b) upper Dudhkoshi catchment, respectively. The corresponding monthly observed SW_{in} for Chandra (upper Dudhkoshi) catchment was shown by red lines + symbols (blue lines + symbols). In Chandra (upper Dudhkoshi) catchment the correction factor used was 2.1 (0.71).

Table S2. The values of the model parameters used in simulations.

Parameter	Description	Range	Value used here
VIC model parameters (https://vic.readthedocs.io/en/master/)			
Ds_{max} (mm day^{-1})	Maximum velocity of baseflow	10–20	15
Ds	Fraction of Ds_{max} where nonlinear baseflow begins	0.1–0.5	0.35
Ws	Fraction of maximum soil moisture where nonlinear baseflow occurs	0.4–1.0	0.7
b_{inf}	Variable infiltration curve parameter	0.001–0.100	0.050
T_{th} (°C)	Threshold temperature for rain-snow partitioning	−1.0–1.0	0.0
Glacier runoff (Hannah and Gurnell, 2001)			
K_{fast} (hr)	Storage constant for fast reservoir	1–24	12
K_{slow} (hr)	Storage constant for slow reservoir	500–2000	1200
Routing model (Lohmann et al., 1998)			
UH^F_{max} (hr)	Unit hydrograph for fast flow	0.5–4.0	2
UH^F_{pow}	Parameter for shape of fast flow unit hydrograph	2–6	4
Bf (hr)	Storage constant for slow flow	1000–3000	2000
Ks (hr)	Storage constant for fast flow	100–1000	550

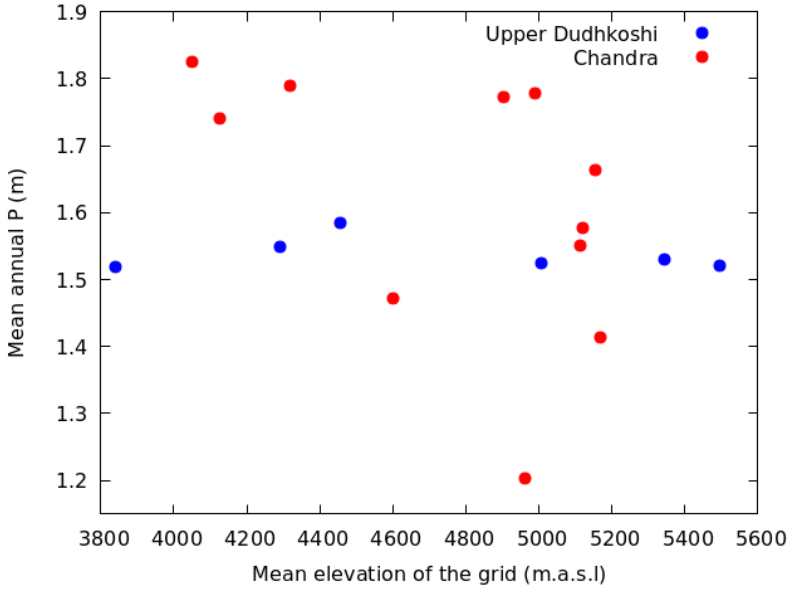

Figure S4. In Chandra and upper Dudhkoshi catchments, the mean annual precipitation of individual gridboxes are plotted against mean elevation of the corresponding gridbox.

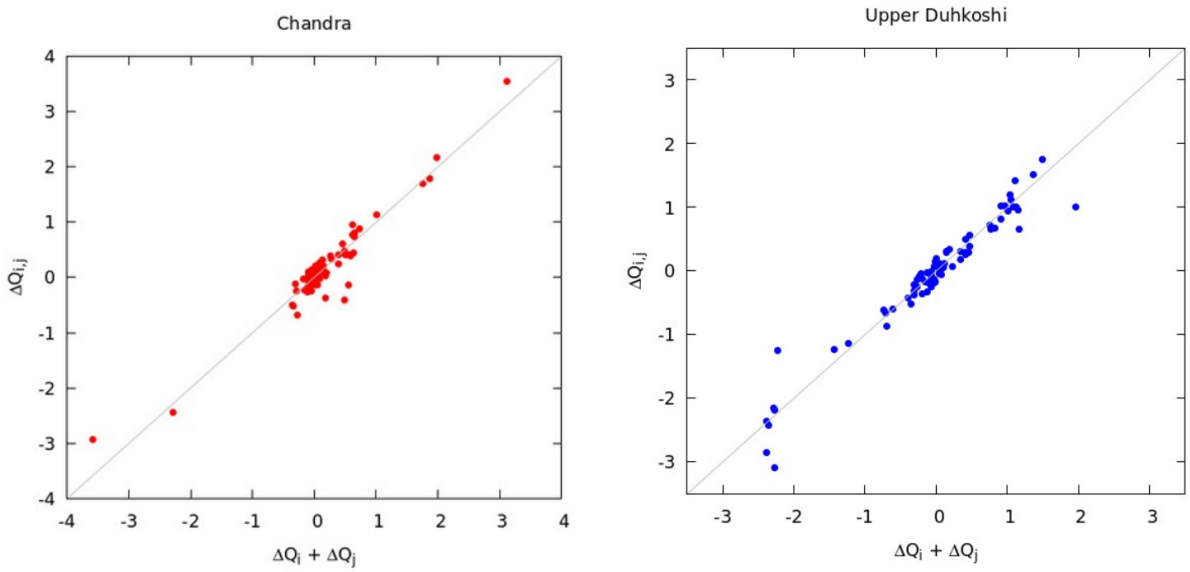

Figure S5. Percentage changes in runoff ($\Delta Q_{i,j}$) in 80 model runs, where two randomly chosen parameters out of the 11 VIC model parameters were perturbed simultaneously, are plotted against the sum of the runoff changes ($\Delta Q_i + \Delta Q_j$) from two corresponding experiments where only one of the two parameters were perturbed.

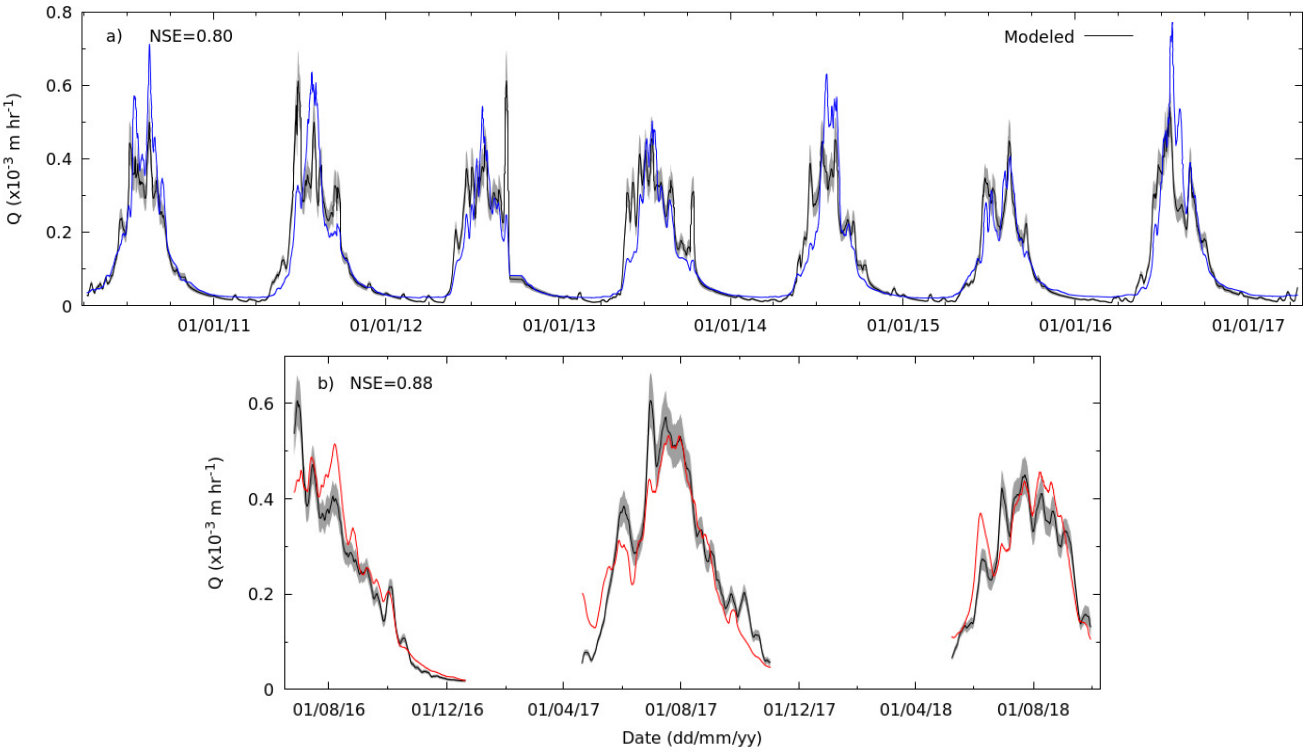

Figure S6. Figure shows the sensitivity of the model results to model parameters. The solid black line shows the best-fit modelled weekly runoff for (a) upper Dudhkoshi, and (b) Chandra catchments. The grey band shows the 2-σ uncertainty band, which were estimated using an ensemble of 200 models where one of the randomly chosen among the 13 model parameters (11 model parameters and two calibration parameters) perturbed by $\pm 25\%$. The corresponding observed weekly runoff for upper Dudhkoshi (Chandra) catchment was shown by blue (red) solid line.

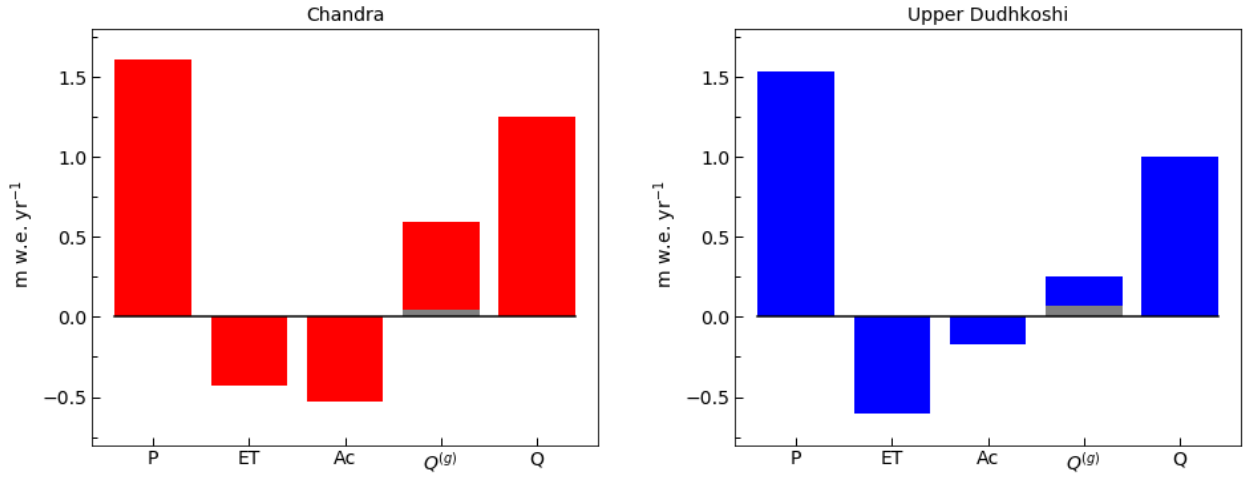

Figure S7. The components of annual hydrological balance equation $P - ET - Ac + Q^{(g)} = Q$ are shown for the two catchments. All the components are normalised by the total catchment area. P, ET, Ac, $Q^{(g)}$, and Q are the annual precipitation, evapotranspiration, glacier accumulation, the runoff from glacerised area, specific runoff from whole catchments, respectively. The imbalance contributions of the glaciers are also shown with grey bars.

Table S3. A comparison of modelled glacier mass balance with the available regional geodetic mass balance for both the catchments. For the modelled mass balance values marked with *, the modelled mean were computed starting from the year 1980. The observed geodetic mass balance values marked with † refers to corresponding catchment values, and the remaining regional values correspond to Lahul-Spiti (for Chandra catchment) and Everest/Khumbu (for upper Dudhkoshi catchment) regions.

Period	Mean modelled mass balance (m w.e yr^{-1})	Geodetic mass balance (reference) (m w.e yr^{-1})
	Chandra catchment	
1980–2018	-0.18 ± 0.10	
1980–1992	0.29 ± 0.18	
1993–2018	-0.42 ± 0.14	
1975–2000	$-0.05\pm0.11^*$	-0.13 ± 0.14 (Maurer et al., 2019)
2001–2016	-0.32 ± 0.12	-0.48 ± 0.15 (Maurer et al., 2019)
2000–2012	-0.40 ± 0.19	-0.52 ± 0.32 (Vijay and Braun, 2016)
2000–2015	-0.41 ± 0.16	-0.30 ± 0.10 (Mukherjee et al., 2018)
2000–2016	-0.41 ± 0.16	$-0.37\pm0.09^\dagger$ (Brun et al., 2017)
		$-0.31\pm0.08^\dagger$ (Shean et al., 2020)
1999–2011	-0.49 ± 0.20	-0.45 ± 0.13 (Gardelle et al., 2012)
		-0.44 ± 0.09 (Vincent et al., 2013)
	Upper Dudhkoshi catchment	
1980–2018	-0.37 ± 0.04	
1980–1992	-0.19 ± 0.07	
1993–2018	-0.46 ± 0.05	
1975–2000	$-0.29\pm0.06^*$	-0.29 ± 0.05 (Maurer et al., 2019)
1970–2007	$-0.31\pm0.05^*$	-0.31 ± 0.08 (Bolch et al., 2011)
2001–2016	-0.44 ± 0.05	-0.39 ± 0.06 (Maurer et al., 2019)
2000–2016	-0.44 ± 0.05	$-0.33\pm0.32^\dagger$ (Brun et al., 2017)
		-0.52 ± 0.22 (King et al., 2017)
		$-0.43\pm 0.25^\dagger$ (Shean et al., 2020)
1999–2011	-0.41 ± 0.06	-0.26 ± 0.13 (Gardelle et al., 2012)
1992–2008	-0.43 ± 0.06	-0.42 ± 0.30 (Nuimura et al., 2012)

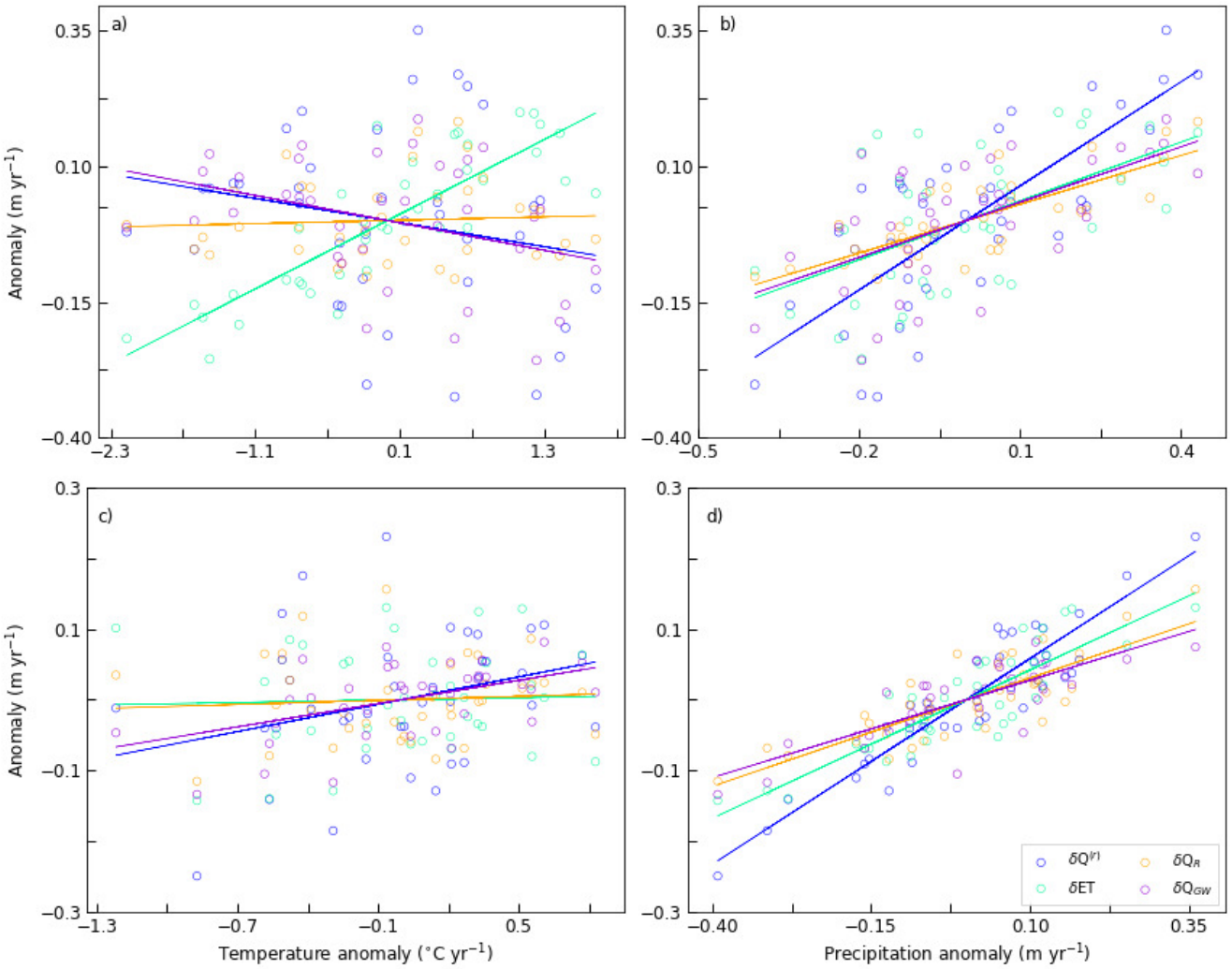

Figure S8. The anomalies of glacier off-runoff ($\delta Q^{(r)}$), and its components, surface runoff (δQ_R) and groundwater/baseflow (δQ_{GW}) are plotted here. The corresponding evapotranspiration (δET) anomalies are also shown. (a)–(b) are the plots for Chandra catchment, and (c)–(d) for upper Dudhkoshi catchment, respectively.

Table S4. A comparison between the estimated glacier ice melt contribution to annual runoff from this study and that of from the available literature.

Study area	Glacerised fraction	Reference	% of glacier ice melt contribution to annual runoff
Chandra catchment	0.25	This study	31 ± 11
Chhota Shigri glacier	0.50	Azam et al. (2019)	18 ± 3
		Engelhardt et al. (2017)	33 ± 4
Upper Dudhkoshi catchment	0.20	This study	32 ± 9
Dudhkoshi catchment	0.13	Nepal (2016)	5
		Chandel and Ghosh (2021)	8
Periche catchment	0.43	Mimeau et al. (2018)	45

Table S5. Percentage sensitivity values for both the studied catchments are given below.

Sensitivity parameter	Chandra catchment	Upper dushkoshi catchment
Catchment summer runoff sensitivities		
s_T (% of Q change per °C warming)	11±1	14±4
s_P (% of Q change due to 10% change in P)	6±1	9±1
Glacier and off-glacier summer runoff sensitivities		
$s_T^{(g)}$ (% of Q change per °C warming)	37±2	58±7
$s_T^{(r)}$ (% of Q change per °C warming)	2±1	3±5
$s_P^{(g)}$ (% of Q change due to 10% change in P)	-2±1	0±0
$s_P^{(r)}$ (% of Q change due to 10% change in P)	9±1	9±1

Table S6. Comparison of our estimates of catchment runoff sensitivities with that of reported in the Himalaya and elsewhere.

Catchment name	s_T (% of Q change per °C warming)	s_P (% of Q change due to 10% change in P)	Reference
Engabreen	24	2	Engelhardt et al. (2015)
Ålfotbreen	17	6	Engelhardt et al. (2015)
Nigardsbreen	21	4	Engelhardt et al. (2015)
Storbreen	19	3.3	Engelhardt et al. (2015)
Ala-Archa	9	7	He (2021)
Dokriani	20	16	Azam and Srivastava (2020)
Dudhkoshi	5	10	Pokhrel et al. (2014)
Trambau	27	-0.6	Fujita and Sakai (2014)
Chandra	11±1	6±1	This study
Upper Dudhkoshi	14±4	9±1	This study

Table S7. Comparison of our estimates of climate sensitivity of glacier runoff with that of reported in the Himalaya and elsewhere.

Catchment name	$s_T^{(g)}$ (% of Q change per °C warming)	$s_P^{(g)}$ (% of Q change due to 10% change in P)	Reference
Midtre Lovenbreen	55	1	Pramanik et al. (2018)
Kongsvegen	71	3	Pramanik et al. (2018)
Kronebreen-Holtedahlfonna	55	4	Pramanik et al. (2018)
Brewster glacier	60	4	Anderson et al. (2010)
La Paz, Bolivia		6	Soruco et al. (2015)
Trambau	53	-7	Fujita and Sakai (2014)
Chandra	37 ± 2	-2 ± 1	This study
Upper Dudhkoshi	58 ± 7	0 ± 0	This study

Table S8. A comparison of glacier mass balance sensitivities to temperature and precipitation from this study with those available in the literature.

Catchment	References	Glacier mass balance sensitivity to	
		Temperature (m yr^{-1} $°C^{-1}$)	Precipitation (m yr^{-1}, relative to 10% change in precipitation)
Regional values			
Chandra	This study	-0.47±0.09	0.2±0.04
Chandra	Tawde et al. (2017)	-0.16	0.09
4 western Himalayan glaciers	Wang et al. (2019)	-0.24 to -0.83	0.06 to 0.09
Indus basin	Shea and Immerzeel (2016)	-0.31 to -0.79	
Upper Dudhkoshi	This study	-0.27±0.05	0.05±0.02
Dudhkoshi	Sakai and Fujita (2017)	-0.17 to -0.36	
5 Eastern/central Himalayan glaciers	Wang et al. (2019)	-0.56 to -1.00	0.05 to 0.08
Ganga basin	Shea and Immerzeel (2016)	-0.29 to -0.76	
Western Himalayan glaciers			
Chhota Shigri glacier	Azam et al. (2014)	-0.52	0.16
Shaune Garang, Gor-Garang, Gara, Siachen	Wang et al. (2019)	-0.83, -0.71, -0.71, -0.24	0.06, 0.06, 0.06, 0.09
Central/eastern Himalayan glaciers			
AX010, Changmekhampu, Yala, Tipra	Wang et al. (2019)	-1.00, -0.66, -0.58, -0.56	0.08, 0.06, 0.05, 0.07
Trambau	Sunako et al. (2019)	-0.90	0.18
Dokriani	Azam and Srivastava (2020)	-1.11	0.24

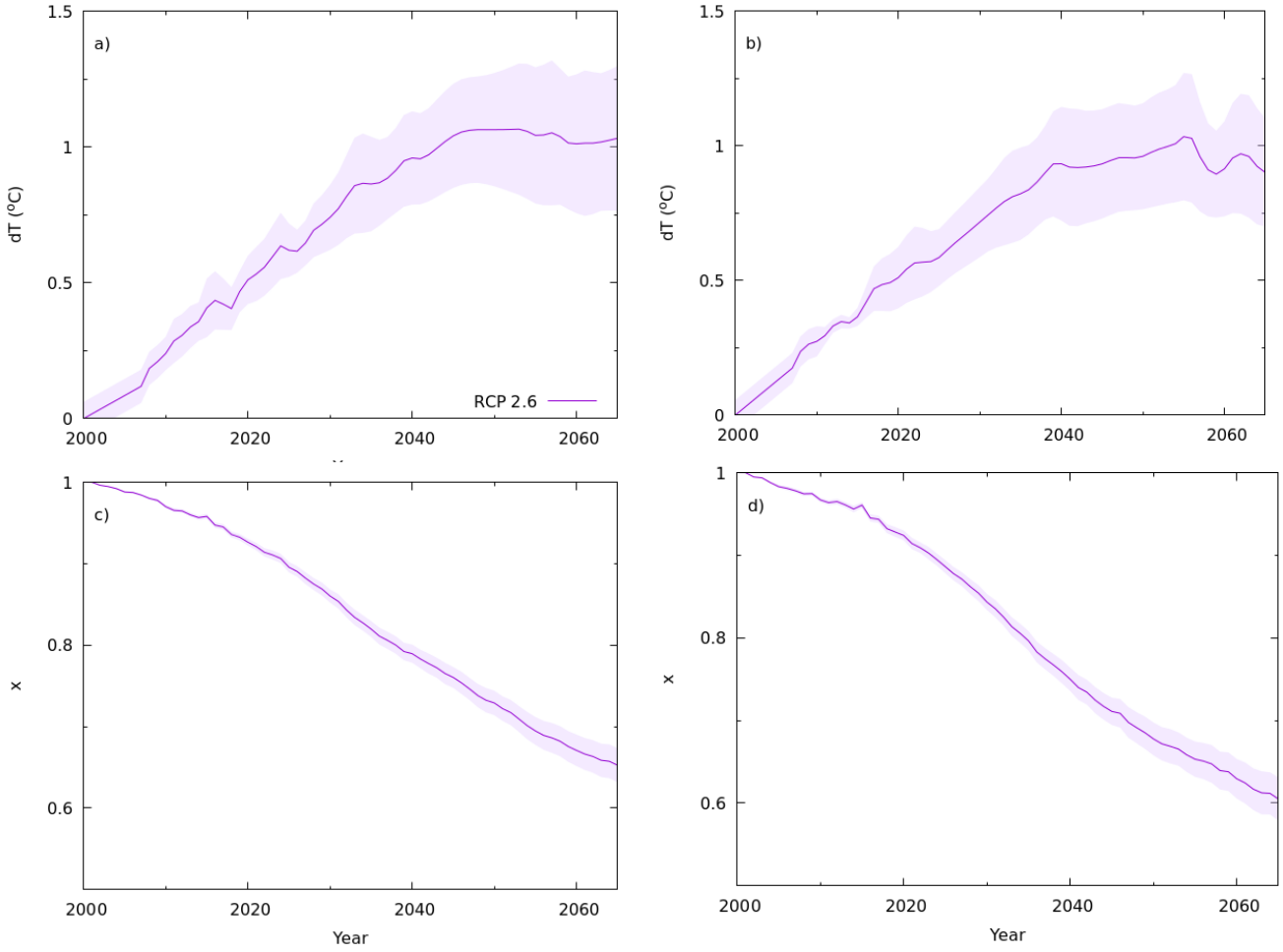

Figure S9. Projected temperature changes over the (a) western, and (b) eastern Himalaya predicted for RCP 2.6 climate scenario (Kraaijenbrink et al., 2017). Kraaijenbrink et al. (2017) provided temperature change data from 2005 onward. Here we extrapolated the data between 2000–2005 using the trend between 2005–2010. Fractional changes in glacier area for (a) Indus, and (b) Ganga basins predicted using RCP 2.6 scenario (Huss and Hock, 2018). In all the four plots, the band is showing the corresponding uncertainties associated with the future projection.